TKK Dissertations 205
Espoo 2009

OPTICAL POSITION DETECTION TO MEASURE TYRE CARCASS DEFLECTIONS AND IMPLEMENTATION FOR VEHICLE STATE ESTIMATION

Doctoral Dissertation

Ari Tuononen

Helsinki University of Technology
Faculty of Engineering and Architecture
Department of Engineering Design and Production

TKK Dissertations 205
Espoo 2009

OPTICAL POSITION DETECTION TO MEASURE TYRE CARCASS DEFLECTIONS AND IMPLEMENTATION FOR VEHICLE STATE ESTIMATION

Doctoral Dissertation

Ari Tuononen

Dissertation for the degree of Doctor of Science in Technology to be presented with due permission of the Faculty of Engineering and Architecture for public examination and debate in Auditorium AS1 at Helsinki University of Technology (Espoo, Finland) on the 7th of December, 2009, at 12 noon.

Helsinki University of Technology
Faculty of Engineering and Architecture
Department of Engineering Design and Production

Teknillinen korkeakoulu
Insinööritieteiden ja arkkitehtuurin tiedekunta
Koneenrakennustekniikan laitos

Distribution:
Helsinki University of Technology
Faculty of Engineering and Architecture
Department of Engineering Design and Production
P.O. Box 4100
FI - 02015 TKK
FINLAND
URL: http://www.edp.tkk.fi/
Tel. +358-9-470 23400
Fax +358-9-470 23419
E-mail: ari.tuononen@tkk.fi

ISBN 978-952-248-249-5
ISBN 978-952-248-250-1 (PDF)
ISSN 1795-2239
ISSN 1795-4584 (PDF)
URL: http://lib.tkk.fi/Diss/2009/isbn9789522482501/

TKK-DISS-2689

Multiprint Oy
Espoo 2009

ABSTRACT OF DOCTORAL DISSERTATION	HELSINKI UNIVERSITY OF TECHNOLOGY P.O. BOX 1000, FI-02015 TKK http://www.tkk.fi

Author Ari J. Tuononen

Name of the dissertation
Optical position detection to measure tyre carcass deflections and implementation for vehicle state estimation

Manuscript submitted 8.9.2009	Manuscript revised 11.11.2009

Date of the defence 7.12.2009

☐ Monograph ☒ Article dissertation (summary + original articles)

Faculty	Faculty of Engineering and Architecture
Department	Department of Engineering Design and Production
Field of research	Vehicle Engineering
Opponent(s)	Prof. Annika Stensson Trigell, Prof. David Crolla
Supervisor	Prof. Matti Juhala
Instructor	Prof. Matti Juhala

Abstract

Future active safety systems for vehicles will need accurate information about the state of the vehicle. Tyre sensors certainly offer an interesting option to evaluate the operating state of an individual tyre. On the other hand, tyre behaviour in some driving conditions is not completely understood and tyre sensor measurements can contribute to the fundamentals of tyre research as well.

This thesis discusses a method to measure the carcass deflection of a rolling tyre. Tyre force estimation algorithms are proposed and tested in real time with a low-cost micro-controller unit. The tyre force information is then exploited to estimate the lateral state of a car. In addition, the tyre sensor signals in aquaplaning are carefully studied and the hydrodynamic and viscous aquaplaning zones were separated from the data in post-processing. Another method was developed to estimate partial and full aquaplaning in real time.

The results obtained support the development of more production-friendly tyre sensor concepts. The relations between carcass deflections and tyre forces that were obtained can be useful for completely different types of sensors. In addition, tyre behaviour in complex conditions can be measured and the results can validate tyre models.

Keywords tyre sensor, optical position detection, active safety systems, vehicle state estimation

ISBN (printed) 978-952-248-249-5	ISSN (printed) 1795-2239
ISBN (pdf) 978-952-248-250-1	ISSN (pdf) 1795-4584
Language English	Number of pages 58 + app. 68

Publisher Helsinki University of Technology, Department of Engineering Design and Production

Print distribution Helsinki University of Technology, Department of Engineering Design and Production

☒ The dissertation can be read at http://lib.tkk.fi/Diss/2009/isbn9789522482501/

VÄITÖSKIRJAN TIIVISTELMÄ	TEKNILLINEN KORKEAKOULU PL 1000, 02015 TKK http://www.tkk.fi

Tekijä Ari J. Tuononen

Väitöskirjan nimi
Optinen paikannus renkaan rungon siirtymien mittaamiseen ja sen hyödyntäminen ajoneuvon tilan estimoinnissa

Käsikirjoituksen päivämäärä 8.9.2009	Korjatun käsikirjoituksen päivämäärä 11.11.2009

Väitöstilaisuuden ajankohta 7.12.2009

☐ Monografia	☒ Yhdistelmäväitöskirja (yhteenveto + erillisartikkelit)

Tiedekunta	Insinööritieteiden ja arkkitehtuurin tiedekunta
Laitos	Koneenrakennustekniikan laitos
Tutkimusala	Ajoneuvotekniikka
Vastaväittäjä(t)	Prof. Annika Stensson Trigell, Prof. David Crolla
Työn valvoja	Prof. Matti Juhala
Työn ohjaaja	Prof. Matti Juhala

Tiivistelmä

Ajoneuvojen aktiiviset turvajärjestelmät tarvitsevat yhä tarkempaa tietoa ajoneuvon tilasta, kuten vaikkapa yksittäisen renkaan toimintatilasta ja olosuhteista. Renkaaseen asennetut anturit tarjoavat tähän oivan vaihtoehdon. Tämän lisäksi rengasantureilla voidaan tutkia renkaan käytöstä yleisemminkin, koska renkaan toimintaa ei kovin hyvin tunneta ainakaan kaikissa ajotilanteissa.

Tässä väitöskirjassa on tutkittu renkaan rungon siirtymien mittausta optisella anturilla sekä tämän tiedon hyödyntämistä. Mitatuista renkaan rungon siirtymistä voidaan laskea renkaan välittämät voimat reaaliajassa. Tätä voimatietoa on edelleen hyödynnetty ajoneuvon sivuttaissuuntaisen liiketilan estimointiin. Tämän lisäksi rengasanturilla tutkittiin vesiliirto-ilmiötä. Vesiliirrossa renkaan kontaktin jakautuminen hydrodynaamiseen ja viskoosiin vesiliirtoon voitiin osoittaa mittaustuloksista. Toinen menetelmä taas kehitettiin arvioimaan osittaista ja täyttä vesiliirtoa reaaliajassa.

Tuloksia voidaan hyödyntää rengasantureiden kehitystyössä. Havaitut relaatiot renkaan rungon muodonmuutosten ja niistä syntyvien voimien välillä ovat hyödyllisiä myös toisenlaisten rengasanturien kehitystyössä, jotka voisivat olla mahdollisia myös tuotteina. Lisäksi rengasanturilla mitattuja tuloksia voidaan hyödyntää renkaan simulointimallien verifioinnissa.

Asiasanat rengasanturi, optinen paikannus, aktiiviset turvajärjestelmät, ajoneuvon tilaestimointi

ISBN (painettu)	978-952-248-249-5	ISSN (painettu)	1795-2239
ISBN (pdf)	978-952-248-250-1	ISSN (pdf)	1795-4584
Kieli	englanti	Sivumäärä	58+ app. 68

Julkaisija Teknillinen korkeakoulu, Koneenrakennustekniikan laitos

Painetun väitöskirjan jakelu Teknillinen korkeakoulu, Koneenrakennustekniikan laitos

☒ Luettavissa verkossa osoitteessa http://lib.tkk.fi/Diss/ 2009/isbn9789522482501/

Preface

This research was carried out in the Vehicle Engineering Research Group of the Department of Engineering Design and Production at Helsinki University of Technology. The research was mainly funded by the European Commission FRICTI@N project and a scholarship provided by the Faculty of Engineering and Architecture, which are gratefully acknowledged. The main partners were VTT, ika, Nokian Tyres, and Volvo Technology. I would especially like to mention Anssi Rautiainen and Timo Varpula for their pleasant co-operation in improving the tyre sensor technology to this level. Christian Hartweg and Thomas Hüsemann always offered a friendly atmosphere for the discussion of tyre sensors and everything else as well. Mikko Liukkula took care that I always had enough tyres and a test track available. The VTEC team, e.g. Stefan Nord, Fredrik Bruzelius, Johan Casselgren, and Henrik Gildå, made the heavy vehicle implementation of my work possible.

I would like to thank Professor Matti Juhala for giving me the opportunity and encouragement to begin my postgraduate studies. Panu Sainio has always provoked me to go on with venturesome ideas and given me full responsibility to do what I wanted to. Panu gave me permission to fail with my “ideas”, and I have used that chance quite frequently. Thanks for the trust.

I appreciate the contributions of my colleagues and co-authors, especially Lassi Hartikainen and Mika Matilainen, for sharing their ideas and skills with me and publishing our results. My thanks also belong to my friends. They gave me the chance to forget about my work for a moment.

I also want to thank Keijo Kallio for all the milling and drilling and sharing many nice morning coffees with me at the laboratory. Ritva Kähkönen always made things and journeys run smoothly. And when the bureaucracy did not run smoothly, Ritva took care of it. Thank you.

The dissertation would not be possible in this form without Pekka Martelius. I want to thank Pekka for designing the tyre sensor components, keeping the data acquisition running, and fixing all the electrics that I all too often broke.

I would like to thank my mother Raila and sister Tarja for encouraging me and, on the other hand, for keeping my feet on the ground. My father has always been an example for me and his memory has pushed me forward every single day.

Finally, I want to thank my wife Johanna and my sweet daughter Minttu for their love and support.

Ari Tuononen

Espoo, November 17, 2009

Contents

List of Publications

This thesis consists of an overview and of the following publications, which are referred to in the text by their Roman numerals.

I Tuononen, Ari. J., "Optical position detection to measure tyre carcass deflections", Vehicle System Dynamics, Vol. 46, No. 6, pp. 471 – 481, 2008

II Tuononen Ari J., Lassi Hartikainen, "Optical position detection sensor to measure tyre carcass deflections in aquaplaning", Int. J. Vehicle Systems Modelling and Testing, Vol. 3, No. 3, pp. 189 – 197, 2008

III Tuononen, Ari J., "On-board estimation of dynamic tyre forces from optically measured tyre carcass deflections", Int. J. Heavy Vehicle Systems, Vol. 16, No. 3, pp. 362 – 378, 2009

IV Tuononen, Ari J, Matilainen, Mika J., "Real-time estimation of aquaplaning with an optical tyre sensor", Proceedings of the Institution of Mechanical Engineers, Part D: Journal of Automobile Engineering, Vol. 223, No. D10, pp. 1263-1272, 2009

V Tuononen, Ari J., "Vehicle lateral state estimation based on measured tyre forces", Sensors, Vol. 9, No. 11, pp. 8761-8775, 2009

Author's contribution

The author wrote Articles I, III and V. The real-time code in Article III was programmed by Henrik Gildå on the basis of algorithms developed by the author. The measurements, data analysis, and writing of Article II were done equally together with Lassi Hartikainen, but the improved illustrations in the summary are the work of the author. Article IV was written together with Mika Matilainen. The idea of the possible estimation algorithms in Article IV was initiated by the author and implemented in a real-time environment by Mika Matilainen.

List of Abbreviations

ABS	Anti-Blockier-System
ADAS	Advanced Driver Assistance System
ADC	Analogue-to-Digital Converter
APOLLO	Project name: Intelligent Tyre for Accident-free traffic
ASK	Amplitude Shift Keying
CAN	Controller Area Network
CCD	Charge-Coupled Devices
CMOS	Complementary Metal-Oxide Semiconductor
CRC	Cyclic Redundancy Check
DAQ	Data Acquisition
EC	European Commission
ESC	Electronic Stability Control
ESP	Electronic Stability Programme
FEM	Finite Element Method
FPGA	Field-Programmable Gate Array
FRICTI@N	Project name: On-board estimation of friction potential
IMU	Inertial Measurement Unit
LED	Light Emitting Diode
Mbps	Megabit per Second
MCU	Micro-Controller Unit
NHTSA	National Highway Traffic Safety Administration
OTS	Optical Tyre Sensor

PSD	Position Sensitive Detector
RF	Radio Frequency
RWTH	Rheinisch-Westfaelische Technische Hochschule Aachen
TDI	Turbocharged Direct Injection
TKK	Teknillinen Korkeakoulu (Helsinki University of Technology)
VSA	Vehicle Slip Angle
VTT	Valtion Teknillinen Tutkimuskeskus (Technical Research Centre of Finland)

List of Symbols

β	Vehicle slip angle
c	Tyre carcass stiffness-dependent parameters for force estimation
CM	Centroid value of the signal
CM_0	Centre of contact position
CM_{100}	CM value for full aquaplaning
d	Tyre damping-dependent parameters (carcass, tread)
F_z	Vertical force
F_x	Longitudinal force
F_y	Lateral force
G_x	Gain for longitudinal displacement
G_y	Gain for lateral displacement
G_{sum}	Gain for intensity
i	Current of PSD corner
k	Tyre stiffness dependent parameters (carcass, tread)
L	Length of active area of PSD sensor
p_{aqua}	Aquaplaning percentage
V_{sum}	Voltage proportional to intensity of PSD
v_x	Longitudinal velocity
V_x	Voltage proportional to longitudinal displacement of the LED
v_y	Lateral velocity
V_y	Voltage proportional to lateral displacement of the LED
x	Longitudinal displacement of the LED
$\bar{x}$	Mean value of longitudinal displacement
x_{gap}	Amplitude of the longitudinal signal
y	Lateral displacement of the LED
$\bar{y}$	Mean value of lateral displacement
z	Distance of LED from the optical sensor

$\mathbf{z}_{mean}$ Weighted mean of five rotations

List of Figures

1 Introduction

1.1 Background

Active safety systems have become common equipment in all vehicle categories. The introduction of Anti-locking Braking Systems (Anti-blockier-system, ABS) in the 1970s was a milestone, since a computer, rather than the driver, controlled the emergency braking. However, it took more than twenty years until a lateral stability support system, the Electronic Stability Programme (ESP), was introduced. ESP was first used on rear-wheel-driven luxury cars, but the famous Elk test by a Swedish reporter in 1996 expedited the breakthrough of Electronic Stability Control Systems (ESC). During the Elk test a new A-class Mercedes-Benz rolled over, which forced MB to recall all its A-class cars to be fitted with ESP. The reduction in the number of fatal traffic accidents of ESP-equipped cars was quickly noted. Nowadays, the National Highway Traffic Safety Administration (NHTSA) requires all new vehicles in the United States under 4536 kg to be equipped with an ESC system by 2011 because of the remarkable indicated safety benefits [1]. Later, a similar regulation was established by the European parliament for EU countries and all new types of vehicles must be equipped with ESC by 2011 and all new vehicles by 2014 [2].

In future, the development of active safety systems will continue in a more integrated and co-operative direction. In addition to the development of new applications which may improve traffic safety, more accurate information about the operating state of the vehicle and road conditions is also desirable. In existing active systems, e.g. the accelerations and rotational velocities of the vehicle body are measured to derive the vehicle state. But as the tyres transmit all the forces acting on the vehicle except aerodynamic forces and gravity, they are an attractive place to mount sensors to evaluate individual tyre behaviour. Furthermore, it is interesting to measure the tyre contact area, because the global tyre force is generated from the distributed stress in the tread. This stress distribution and its shape and magnitude include information on tyre-road contact conditions, as observed with the pioneering Darmstadt tyre sensor [3].

Therefore tyre sensors are fairly versatile instruments and several potential applications exist. The following different functions of tyre sensors could be listed:

- estimation of friction potential;
- estimation of tyre forces (friction used);
- estimation of wheel speed, slip ratio, and slip angle;
- tyre pressure monitoring;
- the recognition of tyre wear, imbalance etc., and
- the recognition of worn suspension components.

On the other hand, only tyre pressure monitoring can be found from production vehicles. If tyre forces and the friction potential are the main focus of interest, as in this thesis, the following technologies could come into question:

- measuring forces and moments from suspension parts [4];
- measuring deflections of a wheel [5] or wheel bearing [6];
- measuring tyre deflections with a sensor in suspension [7,8] and
- sensor in tyre
    - tread sensor [3, 9, 10, 11]
    - carcass sensor [12, 13, 14, 15, 16].

These different approaches are depicted in Figure 1 and the concepts are described in Article I.

The ability of these technologies to evaluate the operating conditions of tyres depends roughly on the distance from the tyre contact patch. In this context, a sensor in the tyre tread offers the most information but this is a rather aggressive place for a sensor to be mounted. On the contrary, the suspension part strains can be used to calculate tyre forces, but it seems clear that the friction potential, aquaplaning, slip angle, or slip ratio cannot be evaluated with this approach. The phenomena are filtered away before the measurement. Similarly, wheel deflections, wheel bearing deflection, or tyre carcass

sidewalls probably do not contain any other information apart from on the forces that are transmitted. However, sensors that are mounted in the inner liner of the tyre carcass offer many benefits. They are easy to mount and close to the local friction phenomenon. Several different sensor types are studied in the literature, with acceleration sensors being the most popular [e.g. 13, 14]. This thesis concentrates only on an optical tyre sensor, which can be classified as a "carcass sensor". The optical tyre sensor measures the deflection of the tyre carcass with respect to the rim in three dimensions.

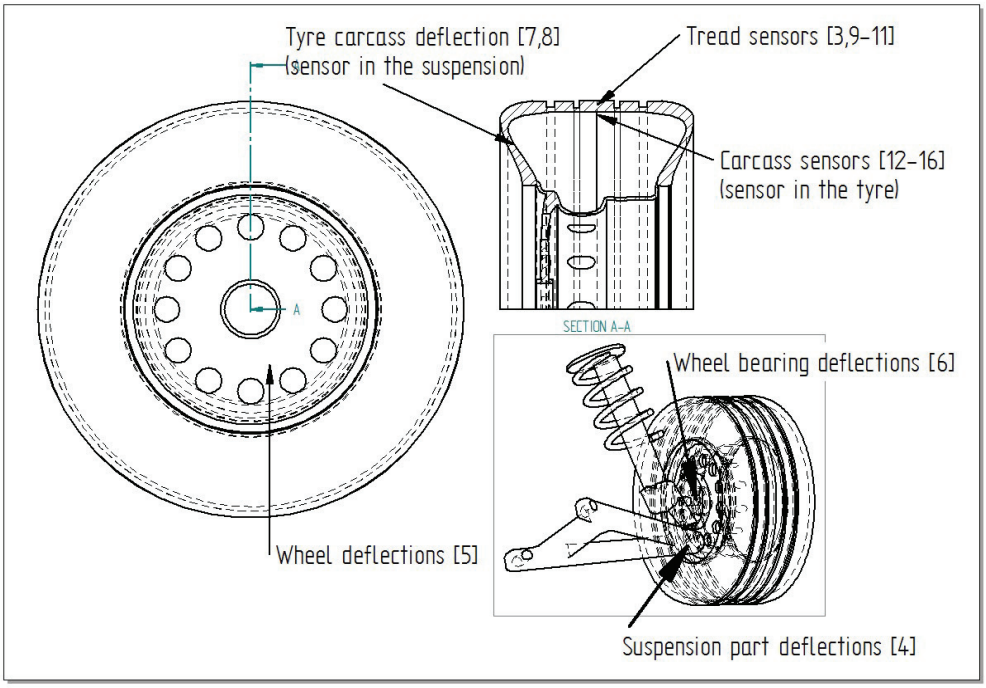

Figure 1 Different tyre sensing concepts

The optical tyre sensor is not designed to be a product, because many of its features are not possible in production vehicles. Thus, the sensor was mainly developed to study the feasibility of tyre force information in active safety systems. In addition, the knowledge of tyre sensors thus acquired is helpful when real production sensors are being considered. All the algorithms developed in this thesis have a strong physical background, so that tyre force estimation is based on tyre carcass stiffness. This allows the same algorithms, or at least ideas, to be exploited when new sensors are being developed.

The results obtained during this thesis project provided the motivation to study tyre behaviour in more detail, especially in conditions that are difficult to simulate and understand. Thus, a very important motivation for the thesis is to explain tyre carcass and contact area behaviour in aquaplaning.

1.2 Summary of publications

Article I explains basic tyre sensor technologies and presents the optical tyre sensor concept. In addition, preliminary algorithms for tyre force estimation were proposed.

Article II studies tyre carcass deflections in aquaplaning. Aquaplaning is traditionally divided into three zones in the contact patch: hydroplaning, viscous aquaplaning, and normal tyre-road contact. The measurement results obtained support this model, in which the standard deviation curves reveal that the hydroplaning zone of contact vibrates and the viscous aquaplaning zone of contact follows the road surface and only a thin layer of water between the tyre and the road prevents the development of frictional forces.

Article III concentrated on a heavy vehicle implementation, because many ADAS applications have been and will be introduced first in heavy vehicles as a result of cost issues and the pronounced safety benefits. Here the optical tyre sensor concept was extended to a truck, and a special rim was manufactured in order to accommodate the sensor module into the tyre. The article presents real-time (16-bit MCU) capable algorithms to estimate the vertical, lateral, and longitudinal tyre forces.

Article IV proposes an algorithm and presents experimental results for the real-time detection of aquaplaning. The interesting results obtained in the post-processing of the aquaplaning data (Article II) encouraged the investigation of recursive methods. There was also motivation to demonstrate the detection of aquaplaning on a proving ground in

a final review of the EC project FRICTI@N. The estimation is based on the shifting of the intensity signal centroid towards the front part of the contact patch. The proposed algorithm is independent of the wheel load and performed reliably with the same parameters in two different types of test cars.

Article V proposed a real application for tyre force information. Vehicle Slip Angle (VSA) estimation has been the subject of numerous research articles. And not without reason: it is the second-state variable of the one-track model, it reveals information about the stability of the vehicle, and it describes whether the driver is still able to control the vehicle by means of steering wheel input [17, 18]. The benefit of the direct force measurement was discussed in Article V and a Kalman filter with an adaptive covariance matrix was proposed in order to estimate the VSA.

1.3 Scientific contribution

The main results of the thesis can be condensed into the following.

1. Rolling tyre carcass deflection relation to generated tyre forces:
    a. quadratic model from amplitude of longitudinal movement to vertical force;
    b. linear model from recursive mean of lateral deflection (of one rotation) to lateral force;
    c. linear model from recursive mean of longitudinal deflection (of one rotation) to longitudinal force.
2. The error detection and force estimation algorithms were modified to be real-time capable in a low-cost 16-bit microcontroller unit (MCU).
3. The transition point from hydrodynamic aquaplaning to viscous aquaplaning in a tyre contact patch was measured from the tyre deflections for the first time. The zones were separated from the intensity and longitudinal movement signals

when the standard deviation of different rotation was calculated in post-processing. The observation supports the existing three-zone model, which explains tyre contact in aquaplaning.

4. Partial and full aquaplaning were estimated in real time.
5. An advanced and novel formulation of the vehicle side slip angle estimation on the basis of measured tyre forces was introduced.

2 An optical tyre sensor (OTS)

The optical tyre sensor consists of an optical position detection sensor and a radio link. These components, with the required specifications, are not commercially available. The tyre sensor in question is not designed for production purposes, but to study tyre behaviour in general and to evaluate the feasibility of tyre sensor information in active safety systems.

2.1 Measurement of tyre carcass deflection

The OTS measures the position of a Light-Emitting Diode (LED) relative to the rim (Figure 2). The LED is glued to the inner liner of the tyre and an optical sensor is mounted on the housing, which is fixed to the rim. The lens focuses the light emitted by the LED onto the surface of the optical sensor. It should be noticed that the radiant intensity of an LED is a function of angular displacement and the alignment of the LED reduces the measured intensity. Consequently, a wide-angle LED was chosen (Vishay VSMS3700) and it was powered with wires from a battery in the sensor module.

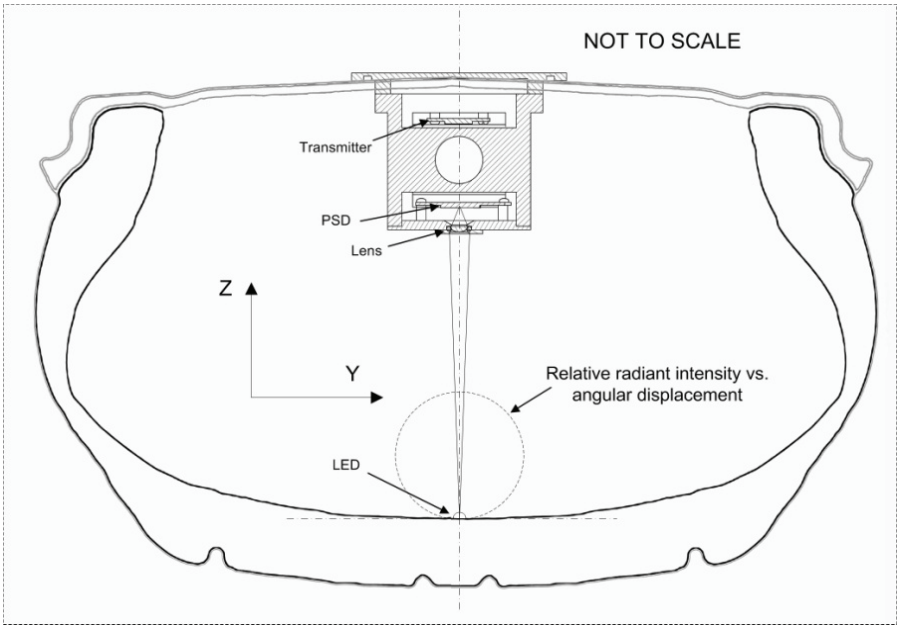

Figure 2 Cross-section of optical tyre sensor (truck version)

The optical sensor is a Position-Sensitive Detector (PSD). In contrast to e.g. Charge-Coupled Devices (CCD) or Complementary metal-oxide semiconductors (CMOS), the PSD is composed of a monolithic detector with no discrete elements. The PSD sensor provides a continuous position data flow by exploiting the surface resistance of the photodiode [20]. Thus, the sensor principle is excellent for tyre sensors, because there is a shortage of energy and the intensive data processing required by matrix sensors is not reasonable in a rolling tyre.

The PSD sensor (Hamamatsu S5991-01 Pin cushion [19]) principle is shown in Figure 3. The active area of the sensor is 10 x 10 mm, the position resolution is 1.5 µm, and the rise time is 2 µs. The light energy is converted into currents (photo sensitivity 0.6 A/W), which are measured from the corners of the sensor. The relative distance of the light source can be calculated thus:

$$z = \sqrt{\frac{1}{\sum i}} \tag{1}$$

and the absolute position in the longitudinal direction:

$$x = \frac{L}{2}\frac{(i_{x2} + i_{y1}) - (i_{x1} + i_{y2})}{i_{x2} + i_{y1} + i_{x1} + i_{y2}} \tag{2}$$

and in the lateral direction:

$$y = \frac{L}{2}\frac{(i_{x2} + i_{y2}) - (i_{x1} + i_{y1})}{i_{x2} + i_{y1} + i_{x1} + i_{y2}} \tag{3}$$

where i is the respective current at the corner of the PSD and L is the length of the active area [20].

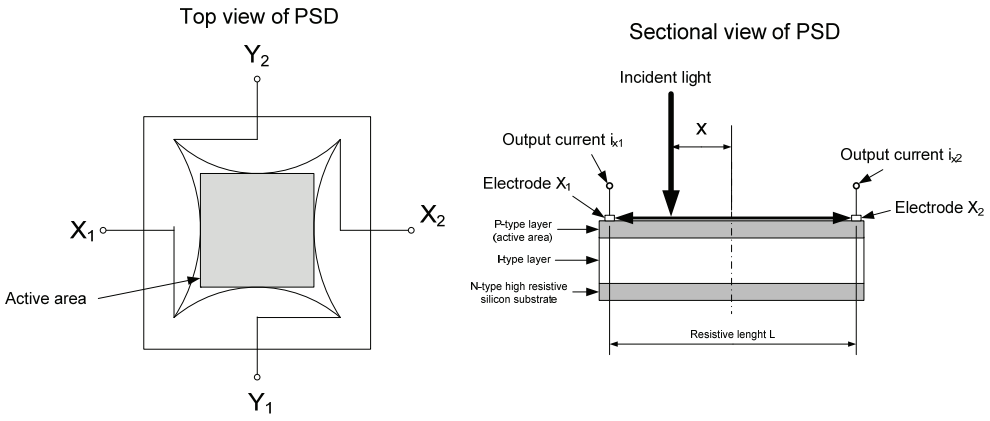

Figure 3 The PSD sensor structure

[principle from 20]

However, the displacements were calculated from a tyre sensor analogue signal with operational amplifiers which executed the equations:

$$V_x = G_x\left[(i_{x2} + i_{y1}) - (i_{x1} + i_{y2})\right] \quad (4)$$

$$V_y = G_y\left[(i_{x2} + i_{y2}) - (i_{x1} + i_{y1})\right] \quad (5)$$

$$V_{sum} = G_{sum}\left[i_{x2} + i_{y1} + i_{x1} + i_{y2}\right] \quad (6)$$

where G is the respective gain to fit the signal to an analogue-to-digital converter. The electrical circuit was manufactured by the Technical Research Centre of Finland (VTT). [21]

The sensor hardware was installed in a separate module, which was mounted on a special rim. In the testing of a passenger car, divisible rims were used to allow the fitting of the tyre after the installation of the sensor. In the truck tyre sensor, a special rim was designed and a hole with a flange joint served as an interface with the sensor module (Figure 4).

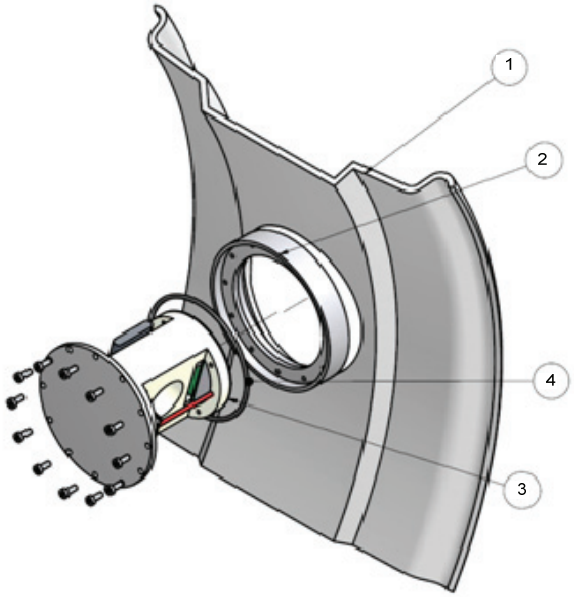

Figure 4 Sensor module installation on the truck wheel rim

(1. rim, 2 flange joint welded to the rim, 3. sensor module, 4. sealing O-ring)

In addition to the optical sensor, a magnetic pickup sensor was installed on the rim and it was aligned with the optical sensor. Naturally, a magnet was installed in the suspension at a location where the optical sensor passed by the top-dead-centre position (Figure 5). This synchronisation signal made it possible to compare OTS signals from different rotations reliably and reproducibly.

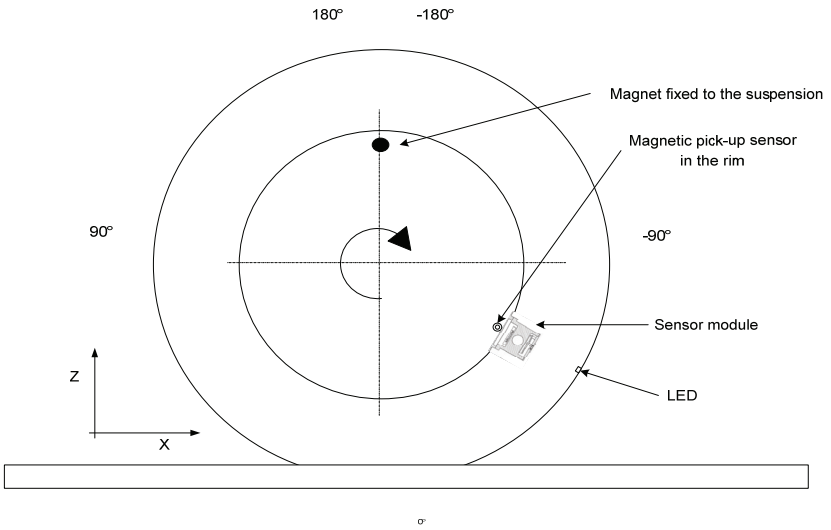

Figure 5 Optical tyre sensor components, magnet and magnetic pick-up sensor

The previously explained measurement setup measures tyre carcass deflections, and not directly the tyre forces acting between the road and the tread. This is explained in Figure 6, where the properties of the carcass and tread are modelled as springs and dampers. The tread is modelled with a spring k_t and a damper d_t. The tread (or inner liner) is connected to a rim with rubber properties k_c and d_c, but the stiffness is dominated by the stiffness k_p generated by the inflation pressure. An important outcome of the model is to observe that the frictional properties of tyre-road contact do not normally have an influence on the measurement of the tyre force with the OTS. In other words, the tyre sensor force estimation can be calibrated in laboratory conditions and the calibration is still valid in completely different frictional conditions. The only assumption is that the carcass properties remain the same and the most important factor is the tyre inflation pressure.

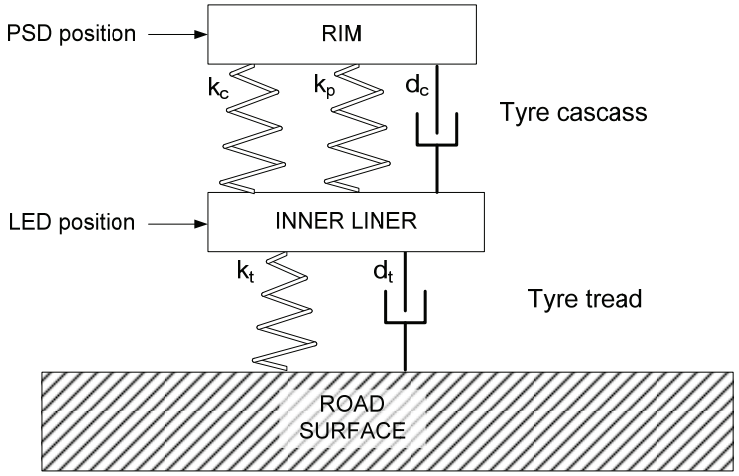

Figure 6 Tyre tread and carcass stiffness and damping properties

2.2 Data transfer

A radio communication device (433.92 MHz) was developed in the APOLLO project [13] and further developed in the FRICTI@N project by the Technical Research Centre of Finland (VTT). The signal flow from the sensor to the vehicle body is presented in Figure 7. The analogue sensor signals are measured with an analogue-to-digital converter (ADC) in the tyre. The sampling rate is 5100 Hz. An 8-bit MCU prepares data

messages, including a Cyclic Redundancy Check (CRC), which is exploited to detect radio errors.

The radio receiver antenna is mounted next to the tyre. The data are demodulated and converted to a CAN message for a high-speed 1-Mbps bus. This receiver unit was developed in the APOLLO project by Magneti Marelli [22].

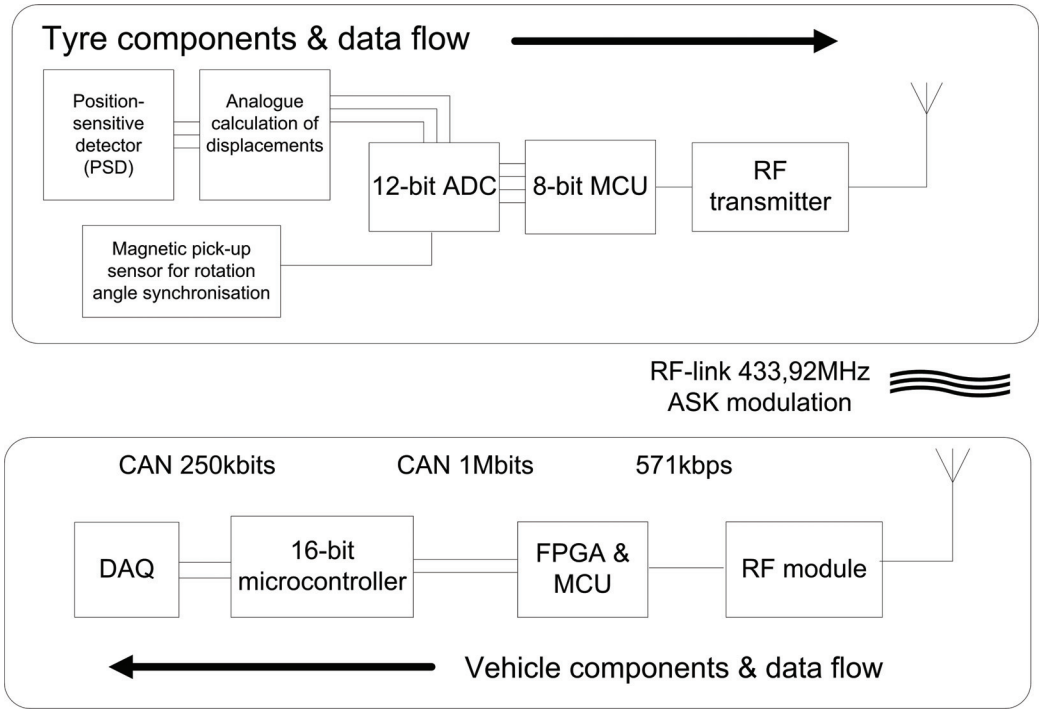

Figure 7 Data flow from tyre to car body

2.3 Raw tyre sensor signals

The simplest of driving conditions is probably driving straight ahead, where the tyre is rolling freely at a constant velocity and load (vertical force). No other forces exist but vertical force and rolling resistance. The OTS signal waveforms in this situation are shown in Figure 8. The units in these figures are not calibrated to a metric scale. The scale is directly the ADC output, which means the range 0-4095 for the 12 bits. The signal intensity is decreasing, even though the LED is coming closer to the sensor during the contact as a result of the inverse configuration of the ADC. A similar peak

during the contact can be seen for the lateral signal, which reveals the mounting offset of the LED, and its compensation is discussed in Article I. The longitudinal signal waveform is strongly affected by the contact deformation of tyre. Before and after the contact the tyre carcass is forced to move away from the contact and zero crossing points are observed at the centre of contact and at the top dead centre. The top-dead-centre position is indicated by the magnetic pickup signal.

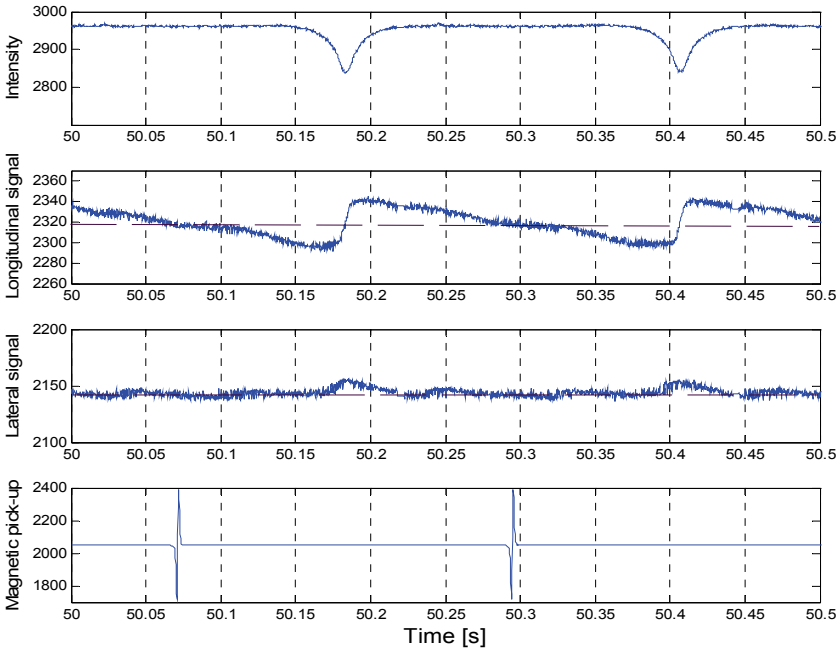

Figure 8 OTS signal in free rolling on chassis dynamometer drum (truck tyre, 50 km/h, vertical load 20 kN)

Figure 9 shows the signals at a constant 6° slip angle, which produces a lateral force of approximately 13 kN at a 30-kN wheel load. The increased wheel load, as compared to Figure 8, can clearly be seen in the intensity signal and in the longitudinal signal. The lateral signal shows how the carcass is stretched during complete rotation and the contact region cannot be observed.

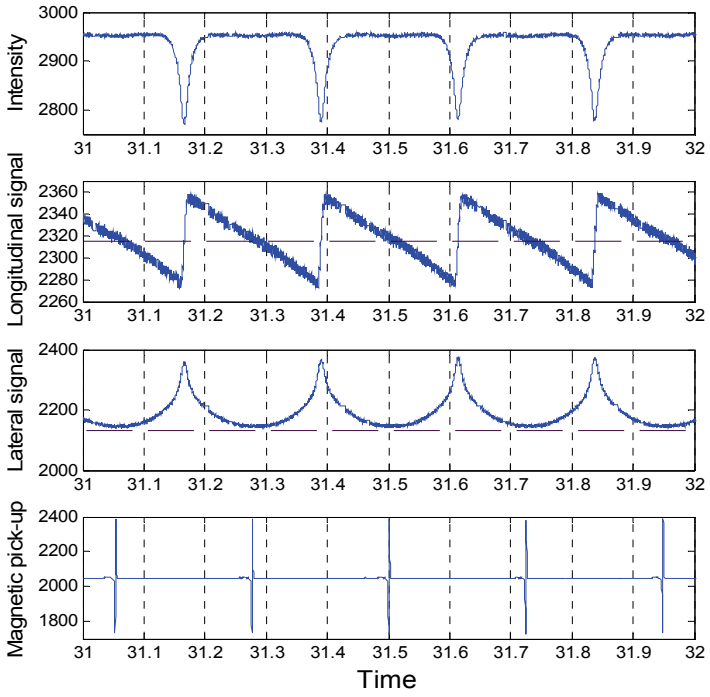

Figure 9 OTS signal at 6° slip angle on chassis dynamometer drum

(truck tyre, 50 km/h, vertical load 30 kN)

2.4 Validation devices

The tyre sensor was exploited to study several different themes, and they needed different validation tools.

The most important tool was a tyre test rig on the chassis dynamometer in the Laboratory of Automotive Engineering of Helsinki University of Technology. The test rig can turn and brake the wheel. Similarly, the wheel load and velocity can be adjusted. In addition, all the forces and moments acting on the tyre can be measured. [23] The test rig had a major role in developing the real-time data transmission and analysis. Another test rig at ika RWTH (Institut für Kraftfahrwesen Aachen) was used for the truck tyre sensor calibrations [24]. The measurements in Article I were performed with a special measurement vehicle owned by Nokian Tyres Plc. In this vehicle, the tyre that was

measured is a “fifth wheel” which can be turned, braked, and accelerated independently. Naturally, the forces and moment are measured simultaneously. [25]

The vehicle measurements in Article III were performed with a Volvo FH12 tractor with a ballast platform. The vehicle slip angle estimation in Article V was developed in a VW Golf V Variant 1.9 TDI. Both vehicles had been modified especially for vehicle testing and equipped with typical vehicle dynamics sensors such as accelerometers and rotational velocity sensors.

The aquaplaning tests were performed at the Nokian Tyres proving ground at Nokia. The test vehicle in Articles II and IV was the same VW Golf as in Article V. The evaluation of aquaplaning was subjective and based on the steering feel of the driver. The differences in the rotational velocities of the front and rear axles confirmed full aquaplaning objectively, but there is no similar method to evaluate partial aquaplaning.

3 Results

3.1 Tyre force estimation (Articles I and III)

The final tyre force estimation algorithms are based on only the longitudinal and lateral displacement signals: the intensity signal is ignored as a result of problems in controlling the intensity of the LED because of variations in temperature, alignment, and battery voltage.

The vertical and longitudinal forces are estimated from the longitudinal signal (Figure 10). Several indicators for the vertical force exist:

- standard deviation of one rotation;
- contact length evaluated from peak values;
- slope of the signal during contact, and
- amplitude of one rotation.

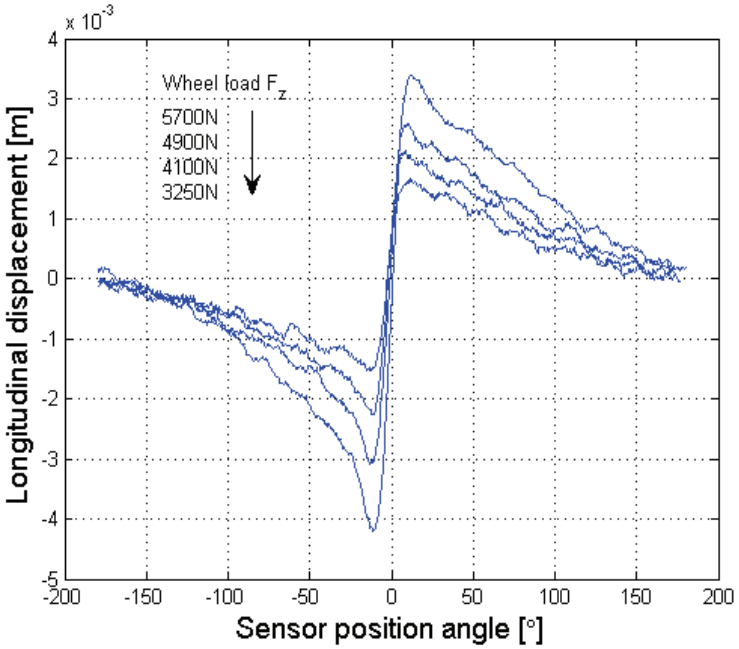

Figure 10 Longitudinal displacement signal as a function of sensor position angle (passenger car tyre)

The standard deviation from the values of one rotation would be very effective against noise in the signal, but a simple model for the estimation of the vertical force was not obtained. The contact length correlates with the vertical force, but it is not possible to determine the position of the peak values accurately. The slope of the signal during contact is sensitive to noise, which is not a particular problem for the sensor in question. However, the signal is not purely linear during contact and then the accurate definition of the contact length appears to be a problem. The algorithm is thus based on the amplitude of the signal:

$$x_{gap} = \max[x_0, x_{end}] - \min[x_0, x_{end}] \quad (7)$$

and where [x_0, x_{end}] includes the longitudinal displacement values of one complete rotation. The vertical force estimate reads:

$$F_z = x_{gap}^2 c_{z,parabolic} + x_{gap} c_{z,gain} + c_{z,offset} + \left[\bar{x} c_{z,x\ gain} + c_{z,x\ offset}\right] \quad (8)$$

with parameters $c_{z,parabolic}$, $c_{z,gain}$ and $c_{z,offset}$. The terms $\bar{x}$, $c_{z,x\ gain}$, and $c_{z,x\ offset}$ are needed to compensate the vertical force estimate under a longitudinal force, which slightly increases the signal amplitude. The tyre sensor estimate is compared to the test rig measurements in Figure 11. The vertical force is slightly overestimated for the low vertical force levels (under 10 kN), but is accurate for the normal operating region of a truck tyre.

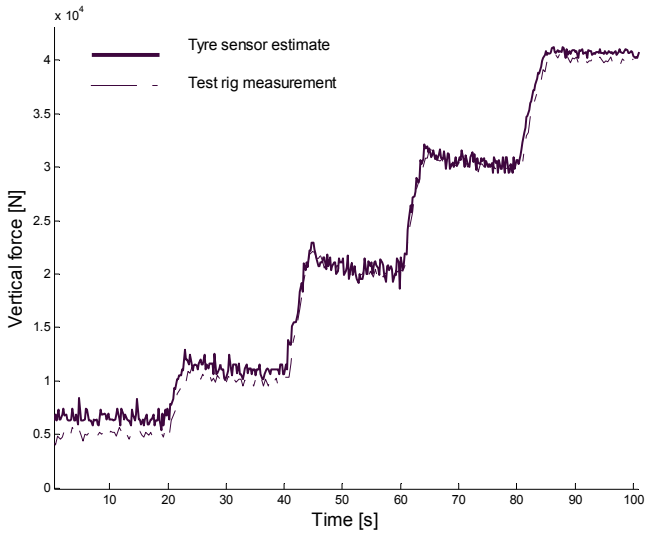

Figure 11 Tyre sensor and test rig comparison for vertical force (truck tyre)

During a longitudinal force, braking or accelerating, the level of the longitudinal deflection signal is changed. An indicator for the longitudinal displacement reads:

$$\overline{x}_{k+1} = \overline{x}_k + \frac{x_{k+1} - \overline{x}_k}{k} \tag{9}$$

and the longitudinal force after one rotation reads:

$$F_x = \bar{x}\, c_{x,gain} + c_{x,offset} \tag{10}$$

with parameters $c_{x,gain}$ and $c_{x,offset}$ and a comparison for the test rig is shown in Figure 12. In the figure, the brake pressure is increased gradually. During the braking testing the tyre temperature increased rapidly, which also increased the inflation pressure and affected the tyre stiffness. If the tyre is stiffer than during the calibration run, the forces are underestimated.

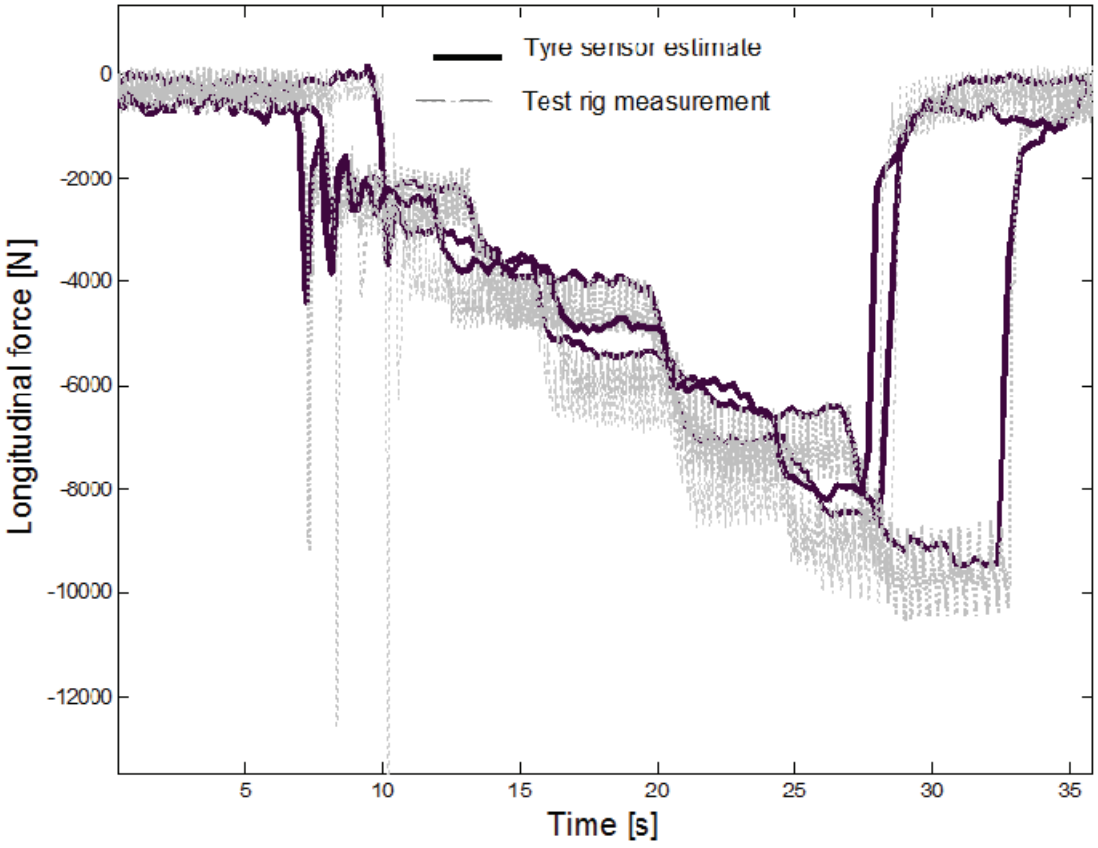

Figure 12 Longitudinal force estimate and test rig measurement for brake steps with different wheel loads (30 km/h, wheel loads 20 kN, 30 kN, and 40 kN, truck tyre)

The lateral signal as a function of the rotation angle is shown in Figure 13. The recursive mean for the lateral deflection of one rotation reads:

$$\overline{y}_{k+1} = \overline{y}_k + \frac{y_{k+1} - \overline{y}_k}{k} \tag{11}$$

and the lateral force reads:

$$F_y = \bar{y}\, c_{y,gain} + c_{y,offset} \tag{12}$$

with parameters $c_{y,gain}$ and $c_{y,offset}$.

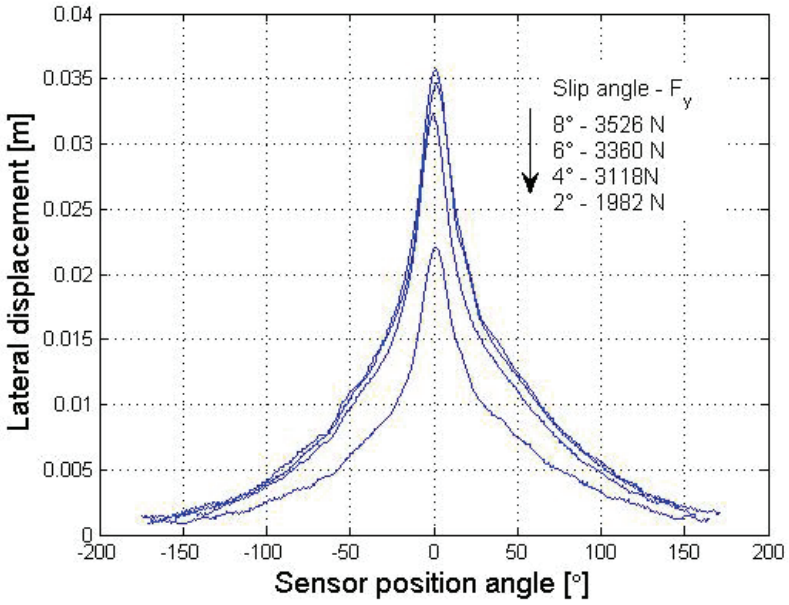

Figure 13 Lateral displacement signal as a function of sensor position angle

The lateral force estimate is compared to the test rig measurements in Figure 14. The estimate is mainly accurate, but some underestimation is observed for the 10-kN vertical load.

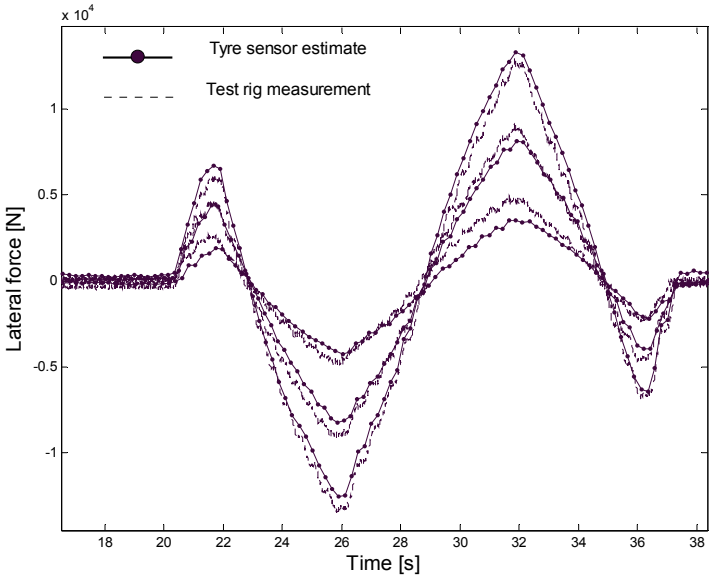

Figure 14 Lateral force estimate from the tyre sensor compared to the test rig measurements (slip angle sweep +-6°, 50 km/h, wheel load 10 kN, 20 kN, 30 kN, truck tyre)

3.2 Estimation of lateral state of vehicle (Article V)

The estimation of the state of the vehicle has been a popular topic for researchers, because information on the lateral state of the vehicle is required by the ESC. The fundamental ideas behind lateral state estimation are presented in [26, 27, 28] and different methods were recently reviewed in [29]. However, even if the existing systems perform under most conditions, more accurate vehicle state information will be needed by future active safety systems such as active steering, lane-keeping support, and torque vectoring. The estimated state is usually the lateral velocity v_y of the centre of gravity of a vehicle. The slip angle of a vehicle is available:

$$tan\beta = \frac{v_y}{v_x} \tag{13}$$

where v_x is the forward velocity of the vehicle.

The main benefit of tyre force-based estimation is that the lateral velocity vector is parallel to the tyre forces. If the estimation is based on traditional lateral acceleration

and yaw rate sensors, the roll angle and road inclination introduce offset to the signals. In particular, the acceleration sensor signal is disturbed by a gravity component.

The proposed estimator was a Kalman filter [30], in which the measurement covariance matrix was adapted according to the driving conditions. The estimator is supported by a linear vehicle model, the operating region of which is limited. In straight-ahead driving the measurement noise variance of the linear single-track vehicle model is adjusted to a very low level compared to the process noise variance. During non-linear vehicle behaviour the measurement noise variance for the linear model is increased and the tyre force integration is consequently weighted. The linearity of the driving conditions is detected from the measured tyre force deviation from the linear estimate of the vehicle model. When there is a difference, the linear model is not accurate any more. The tyre force comparison and corresponding variances for a driving manoeuvre can be seen in Figure 15. The steering angle and lateral acceleration clarify the test manoeuvre and the corresponding lateral force deviation from the linear model can be seen. The lowest plot shows that the measurement noise covariance for the tyre force measurements is constant, but the linear single-track model measurement noise is increased substantially

during slalom driving.

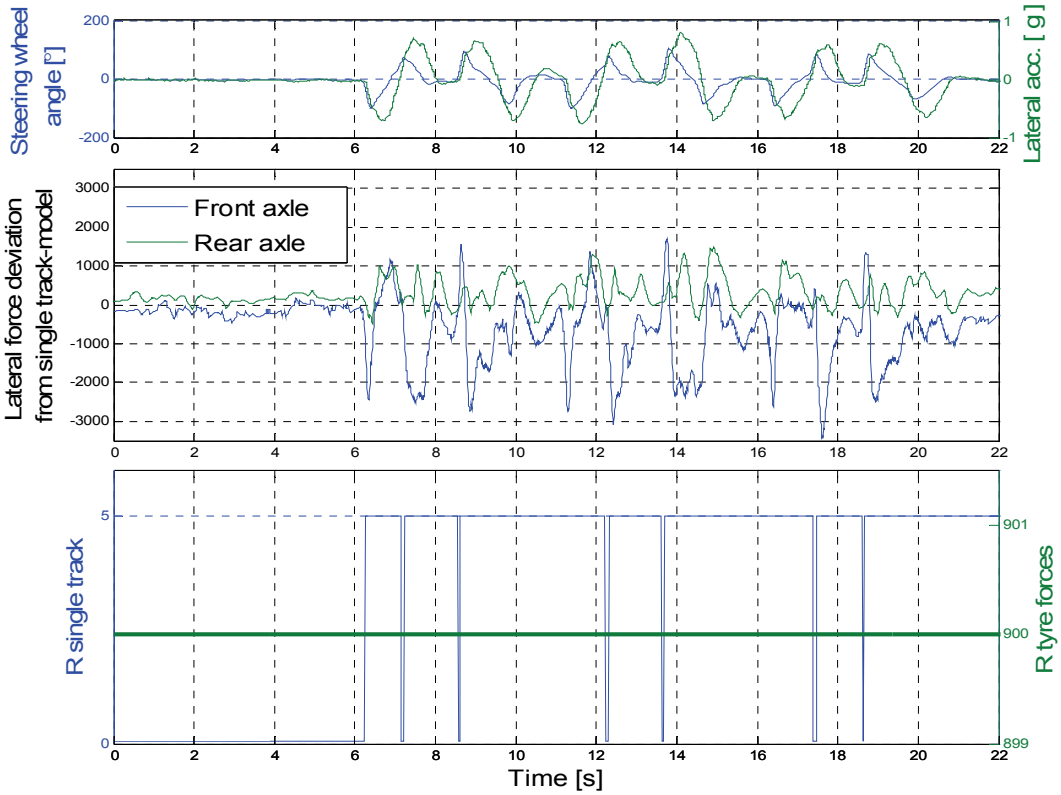

Figure 15 Lateral force deviation from single-track model and measurement error variance during test run

The tyre force-based estimates of lateral acceleration, yaw rate, and lateral velocity are compared to the validation sensor measurements in Figure 16. The yaw rate is slightly overestimated for the positive peak values, which is probably an indication of an overestimated lateral force during a high vertical force. This error cumulates for the negative values of lateral velocity, which can be seen in the lowest plot.

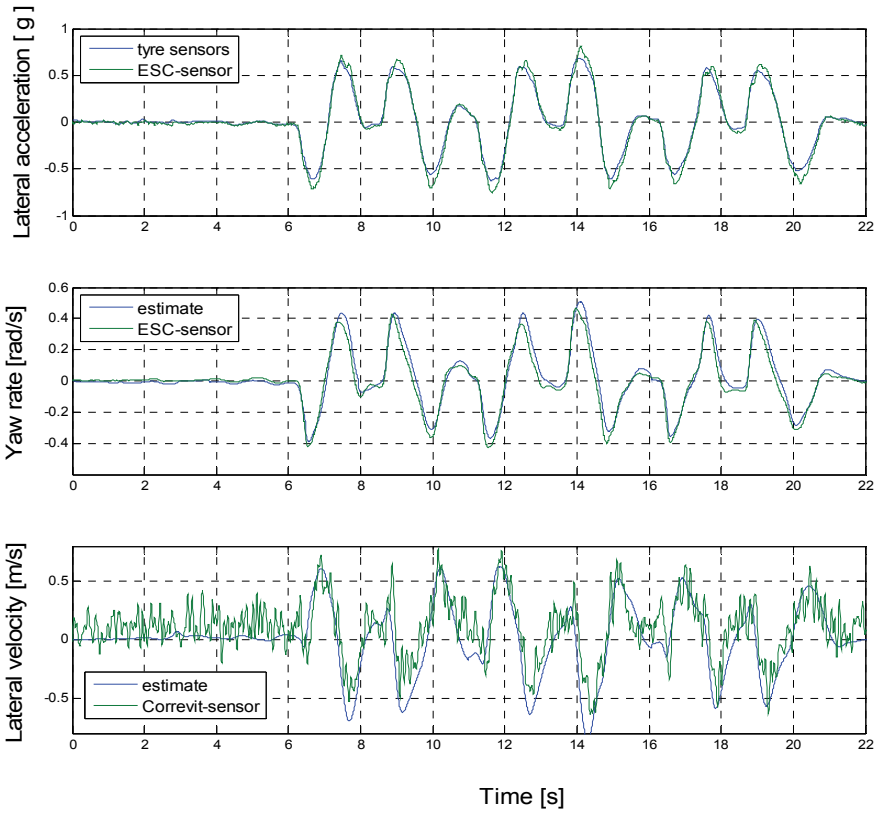

Figure 16 Lateral state estimate based on Kalman filter estimator and for sensor measurement

3.3 Aquaplaning studies (Articles II and IV)

Aquaplaning severely hampers tyre-road interaction. This may lead to a situation where a driver cannot control the vehicle by means of the steering wheel or braking inputs. In addition, if only some of the tyres are aquaplaning, the braking input by the driver may result in a strong and undesired yaw moment. It is obvious that future active systems would benefit from aquaplaning information on individual tyres.

3.3.1 Three-zone model with the Optical tyre sensor (Article II)

The tyre-road contact in aquaplaning has traditionally been divided into three zones [31], which are depicted in Figure 17. The inertial effect of the water dominates in zone

A and no contact between the tyre and the road surface exists. In zone B, some rubber-road contact exists, but the viscous effect of the water squeezing out from the contact area limits this area. Zone C represents normal wet road contact.

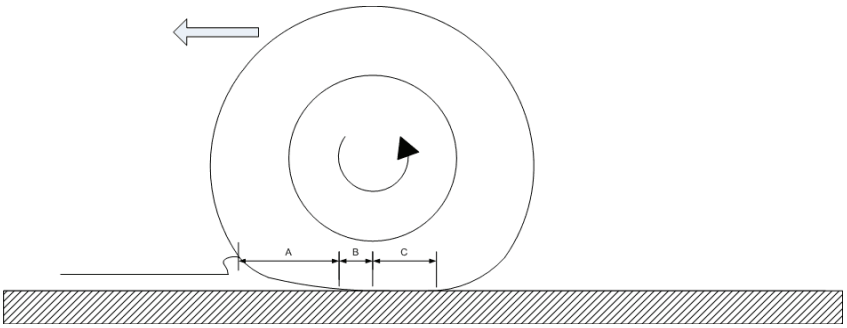

Figure 17 Three-zone concept of aquaplaning tyre

Figure 18 shows the tyre sensor measurement for the transition from dry tarmac to an 8-mm water reservoir. The dry tarmac zone is approximately in rotations 1-55 in the figure, and the water reservoir in rotations 55-74. The left- and right-hand figures relate to the same data; only the view is different. The elevation of the front part of the contact patch can be seen from the increased distance between the LED and the unloaded radius. The signal also shifts slightly towards smaller rotation angles, which can be seen on the right in the figure. The drop in the peak values just before aquaplaning reveals the descent of the tyre into the water reservoir (note arrow in the figure). In other words, it means a reduced vertical tyre force. [32]

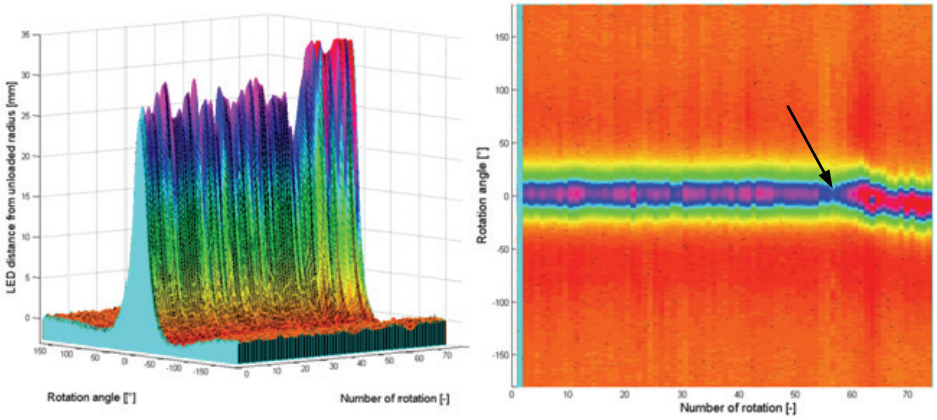

Figure 18 Tyre sensor LED movement on tarmac and on full aquaplaning from [32]

The intensity and longitudinal signals are shown in Figure 19 and Figure 20. The mean values and standard deviations are calculated from ten rotations on tarmac and ten on water. It is suggested that the hydrodynamics zone begins at point A, where the standard deviation of the longitudinal signal diverges from the dry tarmac curve (Figure 20). At the same time, the longitudinal signal minimum is achieved, which also indicates that the contact area is being approached.

Point B separates the hydrodynamic zone from the viscous aquaplaning. Point B can be observed in the standard deviation of both the intensity signal and the longitudinal signal. Before point B, during hydrodynamic aquaplaning, the tyre carcass vibrates as a result of the uneven nature of the inertial forces acting on this area. After point B, the standard deviation curve converges with the dry tarmac curve, which indicates that contact deformation defines the curve. Because of the high velocity and the driver's subjective observation on the proving ground, the tyre is completely without contact with the road in this test. Thus, a probable explanation is that the rear part of the contact, from B to C, is the viscous aquaplaning zone and a thin layer of water separates the tyre from the road. The position of point C lies in the area where standard deviation values settle down to non-contact area values.

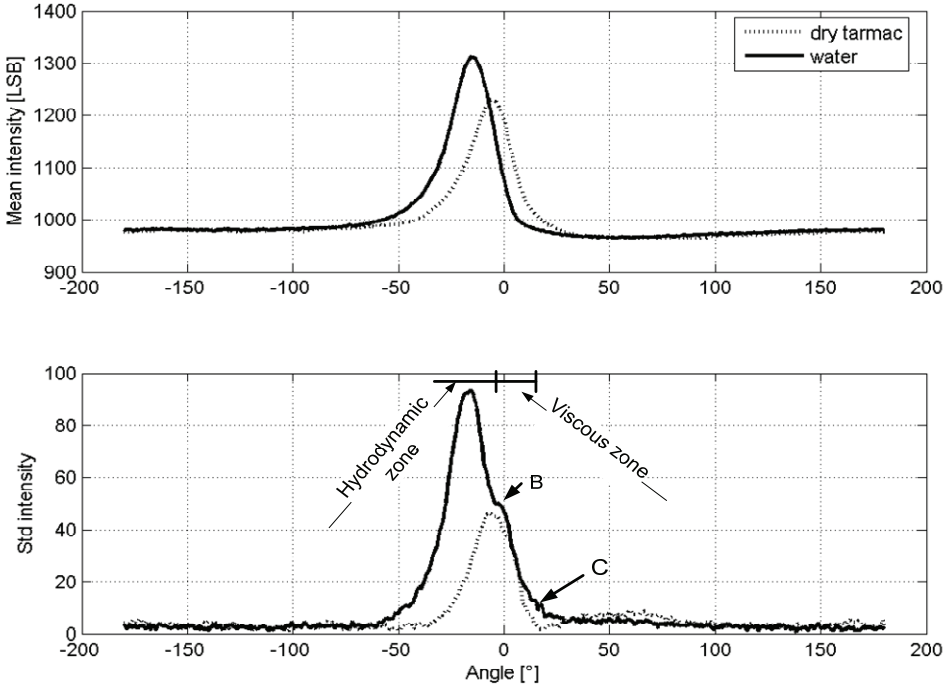

Figure 19 The mean intensity and standard deviation before and after driving into water at 110 km/h

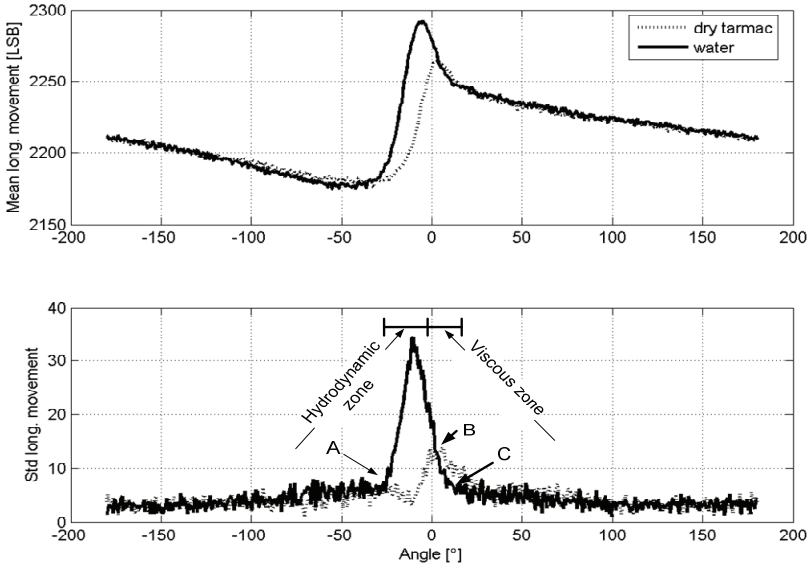

Figure 20 The mean longitudinal movement and standard deviation before and after driving into water at 110 km/h

3.3.2 Real-time aquaplaning estimation (Article IV)

The previous aquaplaning results, where the hydrodynamic zone was separated from the viscous one, were obtained in post-processing. However, it is clear that aquaplaning estimation could aid active safety systems during this uncommon driving situation. The method developed to study aquaplaning in Article II cannot be directly implemented into a recursive form, but the knowledge that was gained about tyre sensor data in aquaplaning encouraged continuation towards real-time estimation.

Several methods for real-time estimation were considered, of which two appeared the most promising:

1. recursive standard deviation of the longitudinal or intensity signal or
2. shifting of the longitudinal or intensity signal for smaller rotation angles could indicate the severity of aquaplaning.

Both methods were tested in real-time conditions and especially method 2, with an intensity signal, performed reliably. It should be noted that both methods are independent of the wheel load, which was an important criterion. Figure 21 shows the measurement data for tarmac and for wet tarmac (aquaplaning condition). The shifting of the signal can clearly be seen.

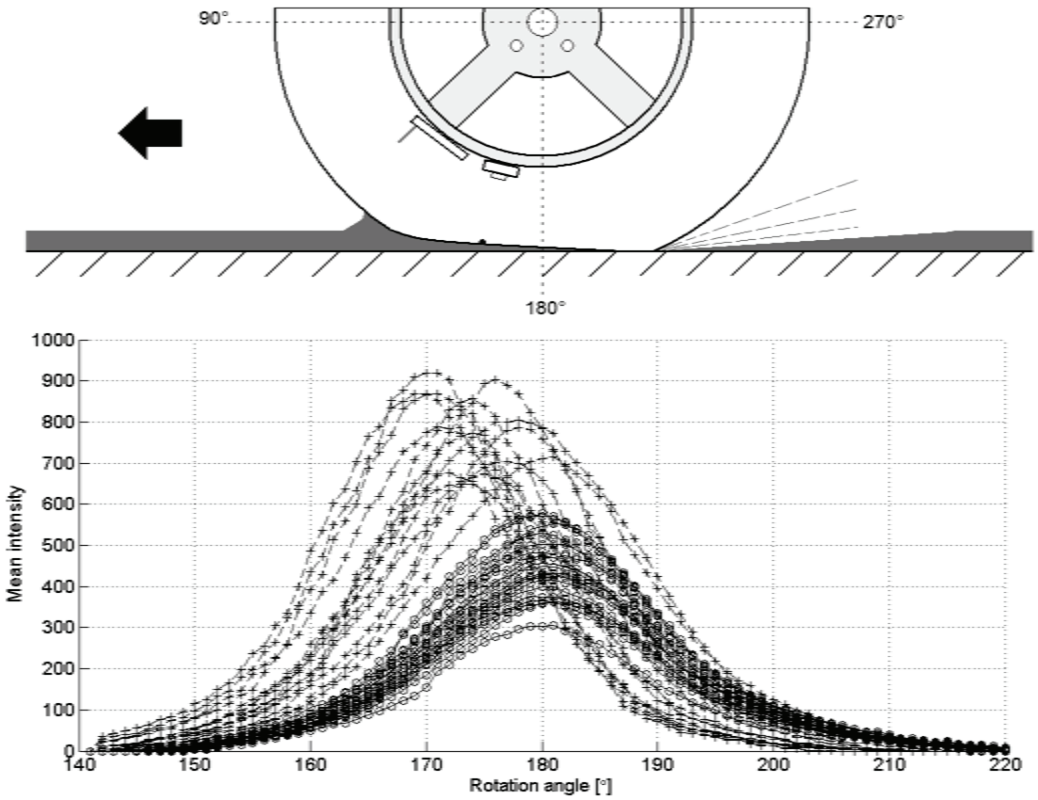

Figure 21 Weighted mean curves of the intensity signal (dry tarmac: lines with circular markers, wet tarmac: lines with plus markers)

In order to compare different rotations, the data are interpolated to the distance domain and the signal is smoothed by calculating the weighted mean $\mathbf{z}_{\text{mean}}$ of five recent rotations. Finally, the centroid of the signal is calculated:

$$CM = \frac{\sum_{i=140}^{220} (z_{mean,i} \cdot i)}{\sum_{i=140}^{220} z_{mean,i}} \tag{14}$$

where only the rotation angles from 140° to 220° are taken into account. The aquaplaning percentage is roughly estimated:

$$p_{aqua} = \frac{100}{(CM_{100} - CM_0)} \times (CM - CM_0) \tag{15}$$

where 100% aquaplaning CM_{100} is defined empirically in the condition where the driver subjectively observed full aquaplaning:

$$CM_{100} \approx 174°$$

$$CM_0 \approx 180°$$

This equation assumes linearity between the centroid values of the signal to aquaplaning contact length, as shown in Figure 22. However, there is no evidence available to validate this assumption.

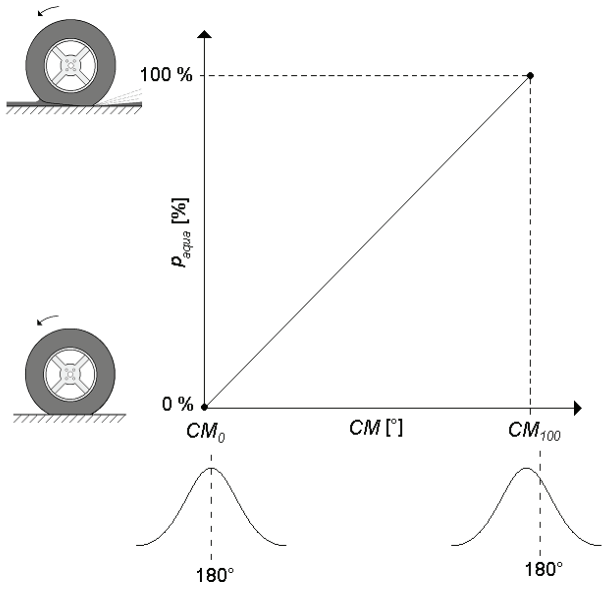

Figure 22 Aquaplaning percentage determination

Figure 23 shows the estimated aquaplaning percentage. The aquaplaning area at the proving ground begins from the zero rotation in the figure. It is interesting to see that partial and not yet dangerous aquaplaning can also be detected for the velocity of 60km/h. The estimated aquaplaning percentage increases gradually with velocity and aquaplaning evolves more quickly at higher velocities (data plotted as a function of rotations).

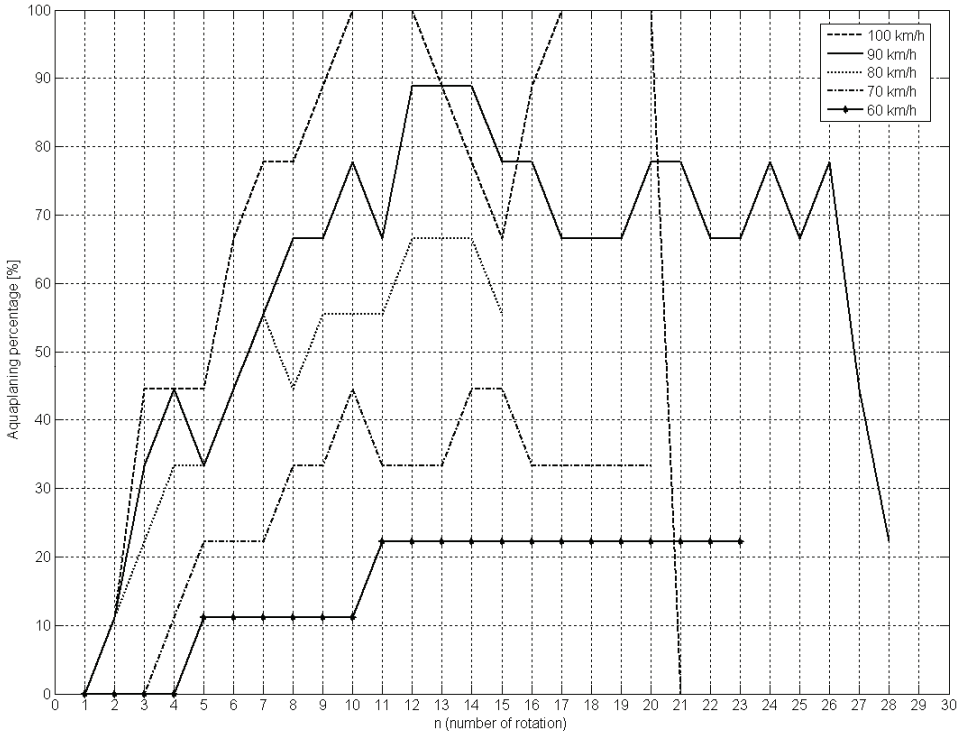

Figure 23 Estimated aquaplaning percentage for different vehicle velocities

4 Discussion

At the beginning of the APOLLO tyre sensor project, the objective was to develop concepts to be ready as a product. However, during FRICTI@N the author forced the research to concentrate more on the fundamentals of tyre behaviour than on modifying components towards mass production. Thus, the intention was to produce information about tyre behaviour that was relevant for the development of tyre sensors. Second, tyre sensors were exploited to study tyre behaviour in complex conditions such as aquaplaning.

4.1 Tyre force estimation

The observed relations between tyre carcass deflections and tyre forces are promising results for more production-oriented concepts. The tyre is a composite construction, in which many properties are very non-linear. A few that can be mentioned are the hyper- and viscoelasticity of rubber, which, in addition, depend on e.g. the compound, temperature, and rate of excitation. Thus, it is not expected that simple and mostly linear models with only a few compensation terms will be able to describe the relation of carcass displacements and tyre forces. The reason for this is probably that the carcass stiffness mostly depends on the air pressure inside the tyre. This dominates over the more complex rubber-ply structure and thus non-linear stiffness and damping properties do not raise their heads. Additionally, the most complex phenomenon in the tyre, friction, is safely away from the inner liner and the carcass just transmits the tread forces to the rim.

The tyre force estimation algorithms should be studied more carefully in the future in combined slip conditions and the tyre force estimation parameters could be inflation pressure-dependent.

4.2 Aquaplaning measurements

The observation in Article II that the viscous aquaplaning zone is rather long in the contact patch raises a question about the Finite Element Method simulations (FEM) of aquaplaning. The FEM does not take into account, at least in its commercial codes, viscous aquaplaning, because the surface roughness is not usually modelled at all. However, the FEM results are rather accurate when compared to the experiments. This would not be expected if almost the half of the contact length is under a phenomenon that is not included in the model. Therefore, it seems that the published knowledge of rolling tyres in aquaplaning is not very comprehensive.

The tyre carcass displacements were exploited to evaluate aquaplaning in real time. Several different levels of partial aquaplaning were detected, in addition to full aquaplaning. The proposed method seems to be accurate, but naturally very sensitive to other phenomena that move the tyre carcass in a longitudinal or vertical direction. One of these situations is when torque is applied to this particular tyre. For example, during braking the vertical signal centroid is shifted in a similar way to what happens in aquaplaning, although the phenomenon is completely different. Hence, the braking situation has to be detected separately, e.g. from brake pressure information, and the aquaplaning information has to be compensated for or ignored during this event.

The real-time algorithm for aquaplaning detection could be modified to reserve less memory if the amount of data vectors is reduced. Additionally, an acceleration sensor or strain sensor measurement in the inner liner of the tyre could effectively measure the vibrating section of the tyre contact patch in aquaplaning and would be a real product application.

It would be interesting to study the influence of inflation pressure on tyre sensor measurements in aquaplaning more carefully, because the inflation pressure affects both the aquaplaning speed and carcass stiffness. Furthermore, the calibration procedure of the tyre sensor could be improved in order to present carcass deflections on a metric scale.

4.3 Slip angle estimation

VSA estimation was presented as an application for tyre force information. However, the main results are presented only qualitatively, not by measurement, because proving grounds offering road inclination and side winds simultaneously are not common. Additionally, the maintenance of the tyre sensor hardware and maintaining valid calibration require test conditions near the home laboratory. Nevertheless, the lateral state of the vehicle was estimated accurately, even if the brilliance of it could not be shown in full scale. The VSA estimation proposed by the author should be extended to cover longitudinal tyre forces as well.

The proposed algorithm is not especially sensitive to vehicle model parameters such as cornering stiffness. However, any offset in the tyre force measurements results, at least, in offset for the lateral velocity estimate. If the one-track model parameters are not accurate, the estimator simply begins to weight the tyre force integration earlier and compensates for this source of error. Meanwhile, an offset error in the tyre force measurement is not compensated for, but results in poor estimates for straight-ahead driving too. Thus, the reliability of tyre force measurements has to be judged separately.

4.4 Future of tyre sensors

The future of tyre sensors is interesting, but probably not very urgent (unlike tyre pressure monitoring). It should be noticed that most tyre sensors require tyre inflation pressure information as an important parameter.

In addition to the technical challenges, the tyre sensor patent situation is complex and may be reflected in the development of tyre sensors. However, many patents may expire before their commercial application is realistic or the patent owner may cease the payment of the annual fee. For example, the well-known Darmstadt tyre sensor seems to be freely available for commercial exploitation [33].

Furthermore, some patents are obviously the results of brainstorming, not of systematic research and development towards future technologies. In particular, some kind of optical tyre sensor is protected by a patent [34], but, as far as author can see, the patent covers only luminous intensity. This releases the optical tyre sensor for the most practical spectrum, the infrared, for the silicon-based optical sensors.

The results in this thesis show that carcass deflections contain interesting information. Optical sensing is not the only method to measure them. Inner liner strain and acceleration sensors can capture the phenomena as well. In particular, aquaplaning could be detected easily with an acceleration sensor because of the vibrating contact patch measured by the OTS.

The tyre sensor research at TKK will continue. Special new rims are being manufactured to allow fast modifications to the sensors without removing the tyre and to expedite experiments with completely new types of sensors. The next step is probably to study carcass deflections more carefully with a laser inside the tyre. The aim is to measure accurately the distance of the inner liner from the rim without the problematic measurement of intensity. It is hoped that this research clarifies whether the friction potential is available from the carcass deflections of a rolling tyre.

References

[1] National Highway Traffic Safety Administration, FMVSS 126, Electronic Stability Control Systems, 2007

[2] Regulation (EC) No 661/2009 of the European and of the Council of 13 July 2009.

[3] U. Eichhorn and J. Roth, Prediction and monitoring of tyre/road friction, Institution of Mechanical Engineers Congress: Safety, The Vehicle and the Road: Technical Papers, Vol. 2, pp. 67-74, FISITA 24th, 7-11 June 1992, London

[4] W.R. Pasterkamp, The Tyre as Sensor to Estimate Friction, Delft University Press, 1997

[5] M. Gobbi and G. Mastinu, Wheels with Integrated Sensors for Measuring Tyre Forces and Moment, AVEC 2004 , 23-27 August, Arnhem, The Netherlands

[6] B. van Leeuwen, F. Pepe: SKF load sensing HBU, ATA Advanced chassis control systems, 2008, Turin

[7] T. Becherer, The Sidewall Torsion Sensor System, 2. Darmstädter Reifenkolloquium, pp. 130-137, 1998

[8] R. Matsuzaki, A. Torodoki, Passive strain monitoring of tyres using capacitance and tuning frequency changes, Smart Mater. Struct. 14, 2005, pp. 561-568

[9] B. Breuer, U. Eichhorn, and J. Roth, Measurement of Tyre/road-Friction Ahead of the Car and Inside the Tyre, AVEC, 1992.

[10] A. Pohl, R. Steindl, and L. Reindl, The intelligent tire utilizing SAW sensors – measurement of tire friction, IEEE Trans. Instrument. Measure. 48(6), 1999, pp. 1041-1046.

[11] O.Yilmazoglu et al., Integrated InAs/GaSb 3D magnetic field sensors for “the intelligent tire”, Sensors and Actuators, A 94, 2001, pp. 59-63.

[12] J. Holtschulze, H. Goertz, and T. Husemann, A simplified tyre model for intelligent tyres, Veh. Sys. Dyn. 43 (suppl), pp. 305-316.

[13] APOLLO, Final report, Available online at: www.vtt.fi/apollo

[14] H. Morinaga, Development of Sensing Algorithm for Intelligent Tire, Tire Technology Expo, Stuttgart, 2006.

[15] V. R. Magori and N. Seitz, On-Line Determination of Tyre Deformation, a Novel Sensor Principle, Ultrasonics Symposium, 1998. Proceedings., 1998 IEEE,Volume 1, 5-8 Oct. 1998, pp. 485-488

[16] J. Holtschulze, Analyse der Reifenverformungen für eine Identifikation des Reibwerts und weiterer Betriebsgrößen zur Unterstützung von Fahrdynamikregelsystemen", PhD thesis, ika RWTH Aachen University, April 2006

[17] Y. Shibahata, K. Shimada, and T. Tomari, Improvement of Vehicle Manoeuvrability by Direct Yaw Moment Control, Proceedings of the International Symposium on Advanced Vehicle Control, AVEC 1992, pp. 452-457

[18] S. Inagaki, I. Kshiro, and M. Yamamoto, Analysis on Vehicle stability in critical cornering using phase-plane method, Proceedings of the International Symposium on Advanced Vehicle Control, AVEC 1994, pp. 287-292

[19] Hamamatsu, Hamamatsu PSD S5991-01 data sheet, 2008

[20] Hamamatsu, Hamamatsu PSD selection guide, 2003

[21] A. Rautiainen, FRICTION PSD ELECTRONICS, internal document, 11.4.2007

[22] A. Nepote et al., The intelligent tyre: A new challenge for automotive electronics, Fisita 2004 World Automotive Congress, Barcelona 2004, 23-27 May

[23] H. Pirjola, Dynamic tyre force measuring device, Helsinki University of Technology, Department of Mechanical Engineering (2002), Available at http://www.tkk.fi/Units/Auto/ 11.8.2009

[24] T. Hüsemann, Tyres in Motion at ika/fka – Tyre Investigations and Research at ika/fka Aachen, First FTire User Meeting, fka Aachen, 17-18 July 2007.

[25] J. Hakanen and T. Kähärä, Tyre characterisation on ice and snow with a measurement vehicle, friction potential and safety: prediction of handling behaviour, 2nd International Colloquium on Vehicle Tyre Road Interaction, Florence, 2001

[26] A.T. Van Zanten, R. Erhardt, G. Pfaff, F. Kost, U. Hartmann, and T. Ehret: Control aspects of the Bosch-VDC, Proceedings of AVEC96, September 1996

[27] Y. Fukada, Slip-Angle Estimation for Vehicle Stability Control, Vehicle System dynamics, 32, pp.375-388, 1999

[28] M. Abe, A. Kato, K. Suzuki, and Y. Kano, Estimation of Vehicle Side-Slip angle for DYC by using On-Board-Tire-Model, Proceedings of the International Symposium on Advanced Vehicle Control, Nagoya, 1998

[29] W.J. Manning and D.A. Crolla, A review of yaw rate and sideslip controllers for passenger vehicles, Transactions of the Institute of Measurement and Control 29, 2007, pp. 117-135

[30] R. E. Kalman, A New Approach to Linear Filtering and Prediction Problems, Transaction of the ASME—Journal of Basic Engineering, pp. 35-45, March 1960.

[31] A. Browne, H. Cheng, and A. Kistler, Dynamic hydroplaning of pneumatic tires, Wear, Vol. 20, pp.1-28, 1972.

[32] A. Tuononen et al., Tyre sensing approach for friction estimation in FRICTI@N project, 17. Aachener Kolloquium, Eurogress Aachen, 6-8.10.2008. Aachen 2008, Institut für Kraftfahrzeuge RWTH Aachen University, 647-658.

[33] Patent number DE3937966, INPADOC LEGAL status, http://fi.espacenet.com, 10.8.2009

[34] Patent number WO0154955 , http://fi.espacenet.com, 10.8.2009

ISBN 978-952-248-249-5
ISBN 978-952-248-250-1 (PDF)
ISSN 1795-2239
ISSN 1795-4584 (PDF)